Using Multiple-Mode Models for Fitting and Predicting the Rheological Properties of Polymeric Melts. II. Single and Double Step-Strain Flows

B. Jiang, P. A. Kamerkar, D. J. Keffer, B. J. Edwards

Department of Chemical Engineering, University of Tennessee, Knoxville, Tennessee 37996-2200

Received 3 October 2005; accepted 16 January 2007
DOI 10.1002/app.26334
Published online 16 May 2007 in Wiley InterScience (www.interscience.wiley.com).

ABSTRACT: Several classes of multiple-mode rheological constitutive equations are examined for predicting the viscoelastic flow properties of a typical polymer melt in single and double step-strain flows. The phenomenological parameters appearing in these models have been obtained by the fitting of experimental data taken in small-amplitude oscillatory shear and steady shear flows. The performance of the models for predicting the experimental data in the step-strain experiments is examined in detail. Specifically, we examine whether or not mode coupling is necessary to describe the experimental behavior under step-strain flows. Furthermore, it is demonstrated that the reversing double step-strain experiment is a very powerful tool for testing viscoelastic constitutive equations. © 2007 Wiley Periodicals, Inc. J Appl Polym Sci 105: 2884–2892, 2007

Key words: melt; modeling; rheology; viscoelastic properties

INTRODUCTION

For many years, the overriding goal of theoretical rheologists has been to obtain a level of understanding of material behavior sufficient to allow for the prediction of viscoelastic properties in arbitrary flow fields. After many years of effort spent in pursuit of this goal, it is still largely unachieved. In recent years, modeling efforts have intensified as theoretical developments and computational power have increased. It is now timely to reassess, in general terms, the progress made by rheologists toward achieving this goal.

In part I of this study,[1] we presented a current assessment of the potential predictive capabilities of seven viscoelastic fluid models. Rather than focusing on the particular models popular today (which might not be popular a decade from now), we examined instead semiphenomenological models (i.e., models involving empirical parameters) that characterize a certain class of model types. This allowed us to judge the capabilities of the class using the simplest possible methodology; that is, without getting caught up in model-specific peculiarities and complexities.

The strategy of the research reported in this article and ref. 1 is to fit the models examined herein to a limited amount of easily obtained experimental data of a typical polymer melt and then to test how well each quantitatively predicts experimental data to which the inherent model parameters have not been explicitly fit. To accomplish this, we need an extensive suite of experimental data on a single polymer, all taken under the same state conditions (the same temperature, pressure, etc.). Therefore, we focus our attention on a single industrial linear low-density polyethylene (LDPE) polymer melt and obtain experimental data for this melt under the widest variety of flow conditions possible. We believe that these experimental data are very representative of the behavior of many polymer melts, and thus our results are generalizable to other polymers. Furthermore, the rheological behavior of most polymeric liquids is qualitatively independent of the state point of the experiment (i.e., the temperature of the experiment), so experimental data obtained at one temperature can be used to infer those at another—the so-called time–temperature superposition principle.[2]

The model classes examined in the succeeding sections are as follows. The most basic semiphenomenological model class is that of the uncoupled (i.e., no coupling between the various relaxation modes), linear relaxation models with constant relaxation times. The most well known and widely used of these is the multimode upper-convected Maxell model, and thus we examine it herein. Of course, this model has no hope of fitting any nonlinear viscoelastic properties; however, we examine it as a basis for the linear viscoelastic response exhibited by many other models in the linear limit. The second class is that of uncoupled, linear relaxation models with variable relaxation times. Examples of models falling into this group are the Phan-Thien/Tanner model,[3] the modified upper-

Correspondence to: B. J. Edwards (bjedwards@chem.engr.utk.edu).

Journal of Applied Polymer Science, Vol. 105, 2884–2892 (2007)

convected Maxwell model,[4] and the extended White/Metzner model (EWMM).[5] Herein, we examine a version of the EWMM as a representative of this class. The third class is that of uncoupled, nonlinear relaxation models. The example of this class studied herein is the Giesekus model.[6] The remaining two classes of viscoelastic fluid models examined herein are those that involve coupled relaxation modes; that is, the modes are no longer taken to be independent of each other, as is the case in all the examples considered previously. The first remaining class is that of the pairwise coupled relaxation modes models, that is, when each mode is taken to couple to one, and only one, other relaxation mode. The second remaining class is that in which each mode of a given model is allowed to interact with every other mode.

In part I,[1] we examined the performance of seven multimode constitutive equations in small-amplitude oscillatory shear flow (SAOSF), steady-state and transient shear flows, and uniaxial elongational flow. Further information is expected to be obtained through single and double step-strain flows. Single and double step-strain shear flows are convenient and powerful methods for evaluating rheological constitutive equations and examining the coupling effect among the modes in rheological models.[7,8] In a single step-strain experiment, a shear strain of γ is imposed on the test sample at $t = 0$ under the condition that $\gamma = 0$ for $t < 0$. The shear stress, $\sigma(\gamma,t)$, is measured as a function of time. As for a double step-strain experiment, a shear strain of γ_1 is imposed on the test sample at $t = 0$ under the condition that $\gamma = 0$ for $t < 0$; then a second step of strain γ_2 is imposed at $t = t_1 > 0$. The extra stress $\sigma(\gamma_1,\gamma_2,t_1,t)$ is monitored as a function of time.

Descriptions of double step-strain data have been focused on the well-known nonlinear and time-dependent Bernstein/Kearsley/Zappas model[9] and the Doi–Edwards (DE) reptation model.[10] Many studies have led to the similar conclusion that the BKZ model cannot describe quantitatively reversing flows for entangled linear polymers.[11] Venerus and Kahvand[12] carried out a thorough evaluation of DE theory, using the double step-strain flow of monodisperse polystyrene solutions. Also, predictions of several models in reversing shear flows were given by Wagner and Ehrecke.[13] Chodankar et al.[14] examined the integral and differential forms of the pompom model in single and double step strains with respect to the experimental behavior of an LDPE melt. Semianalytical model predictions were also obtained for the stresses in double step-strain shear flows in ref. 14.

The main premise of a double step-strain experiment is the following: a given step strain is applied to a sample, after which the sample begins to relax; after it has partially (but not fully) relaxed, a second step strain is applied to the sample. Hence, right before the application of the second step strain, some of the modes (with short relaxation times) will have completely relaxed, whereas those modes with long relaxation times will not have done so. If all modes are independent, then the long-time modes will have no effect on the short-time modes. However, if mode coupling occurs, some unusual hysteretic phenomena might be observed under certain conditions.

In this part, we use seven different viscoelastic fluid models to predict the stress of step-strain experiments. The performance of these different models in step-strain experiments is examined herein. All theoretical results presented in this article are predictions of experimental data; that is, all parameter fitting was performed in part I[1] for SAOSF and steady shear flow.

EXPERIMENTAL

The polymer studied herein was the same as that described in part I.[1] It was a typical, industrially relevant LDPE sample. The LDPE sample was obtained from Exxon (Newark, NJ). It was prepared with a Ziegler–Natta catalyst. This sample had a wide molecular weight distribution: the value of the polydispersity index was 5.15. Its melt index was 0.2 g/min, with a density of 0.923 g/cm^3. The weight-average molecular weight was 80,350 g/mol, as measured by gel permeation chromatography.

The experiments were conducted with standard rheological testing equipment and procedures at the University of Tennessee. Step-strain measurements of the relaxation stress and the corresponding strain were made on the Advanced Rheometrics Expansion System from Rheometrics Scientific (Newark, NJ) at 175°C. A cone and plate fixture with a 25-mm plate diameter and a 0.1-rad cone angle was used for both single and double step-strain experiments.

COMPUTATIONAL METHODS

A number of multiple-mode rheological models are discussed and examined for the same sample in part I,[1] which presents the corresponding constitutive equations for the rheological models examined: the uncoupled Maxwell modes (UMM) model, the uncoupled extended White/Metzner modes (UEWM) model, the uncoupled Giesekus modes (UGM) model, the pairwise coupled Maxwell modes (PCMM) model, the pairwise coupled Maxwell modes model with the White/Metzner-like extension (PCMM–EWM), the fully coupled Maxwell modes (FCMM) model, and the fully coupled Maxwell modes model with the White/Metzner-like extension (FCMM–EWM model). The parameters of all models were attained by the fitting of experimental data for the

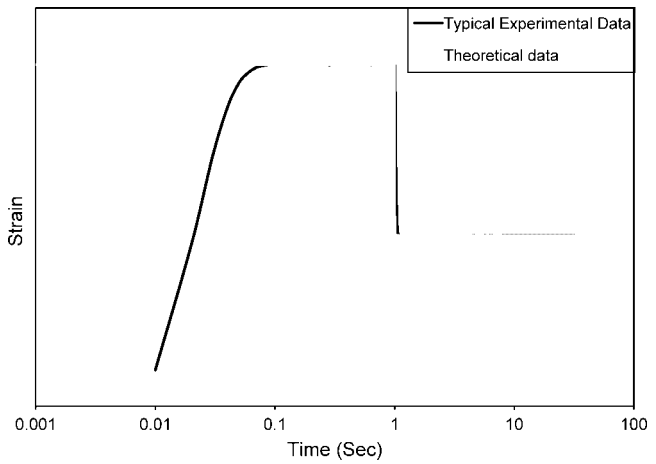

Figure 1 Typical variation, both theoretical and experimental, of the strain with the time in a step-strain shear flow.

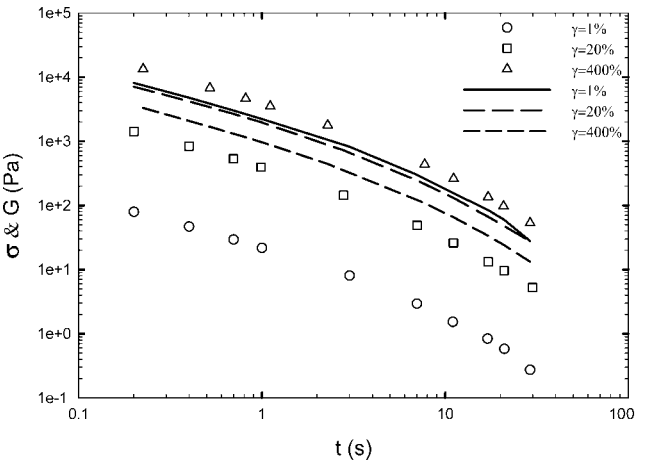

Figure 2 Experimental data for stress σ (symbols) and stress relaxation modulus G (curves) versus time t in single step-strain experiments.

storage and loss moduli in SAOSF and steady shear material functions simultaneously. All the parameters thus obtained are tabulated in part I.[1]

A schematic diagram of the strain versus the time is shown in Figure 1, which demonstrates that, theoretically, an instantaneous strain, γ_0, is applied at time $t = 0$, but experimentally, the rheometer needs a certain amount of time (ca. 0.07 s) to reach the strain required. The corresponding shear rate can be attained through the strain data; therefore, the shear stress can be computed theoretically through the constitutive equations of the different models, as mentioned previously.

In refs. 11 and 15, the stress relaxation modulus, $G(t,\gamma)$, is defined as the ratio of the resulting stress to the step strain: $G(t,\gamma) = \sigma(t,\gamma)/\gamma_0$. We defined $G(t,\gamma)$ as the ratio of the resulting stress to the step strain, $G(t,\gamma) = \sigma(t,\gamma)/\gamma$, because we consider the initial time for the instrument to reach the applied strain, as discussed later.

RESULTS AND DISCUSSION

In the following discussion, only sample results are given. For a full description of all experimental data and model predictions, the reader is referred to ref. 16.

Single step-strain experiments

Figure 2 shows the time dependence of the shear stress and stress relaxation modulus under various step strains. For the applied strains (γ = 1, 20, or 400%), the value of the stress increases quickly and reaches a maximum in less than 0.1 s and then decreases as the polymer melts relax after the strain reaches the value applied. The value of the stress relaxation modulus decreases right after the strain is applied. Single step-strain experiments at lower strain values for the same polymer melts have been examined in detail;[16] these showed that the values of the stress relaxation moduli are not related to the value of strain and that the stress relaxation moduli obey time–strain factorability. At higher values of the applied strain, outside of the linear viscoelastic regime, time–strain factorability broke down.

The prediction of the different models generally agreed with experiment in the low-strain limit. Here, we present the predictions of the FCMM–EWM model as an example, which are shown in Figure 3. As can be seen in the figure, the predictions of the models are generally excellent.

Outside the linear viscoelastic regime, for higher strain values, the different model predictions vary

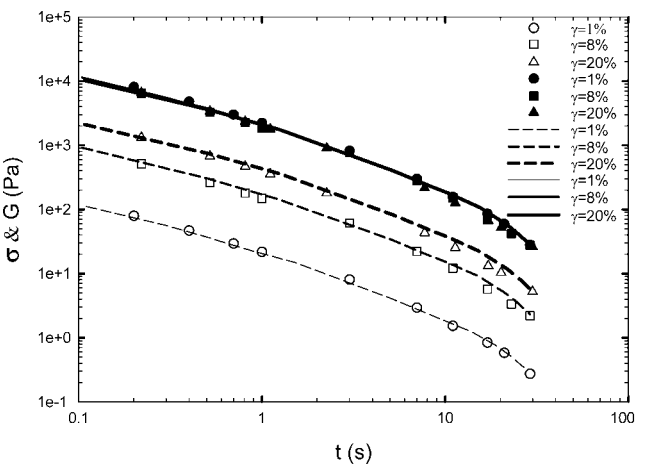

Figure 3 Stress σ and stress relaxation modulus G versus time t, as predicted with the FCMM–EWM model, in single step-strain experiments. Unfilled symbols represent experimental σ data, filled symbols represent G data, continuous curves are model predictions of G, and dashed lines are predictions of σ.

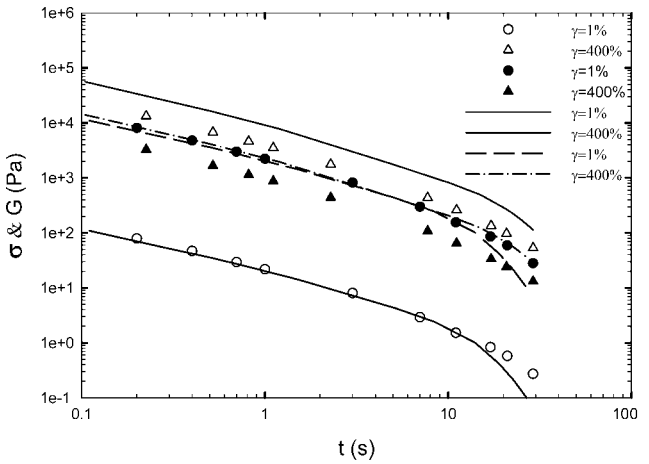

Figure 4 Stress σ and stress relaxation modulus *G* versus time *t*, as predicted with the UMM model, in single step-strain experiments. Unfilled symbols represent σ data, filled symbols represent *G* data, solid lines are σ predictions, and broken lines are *G* predictions.

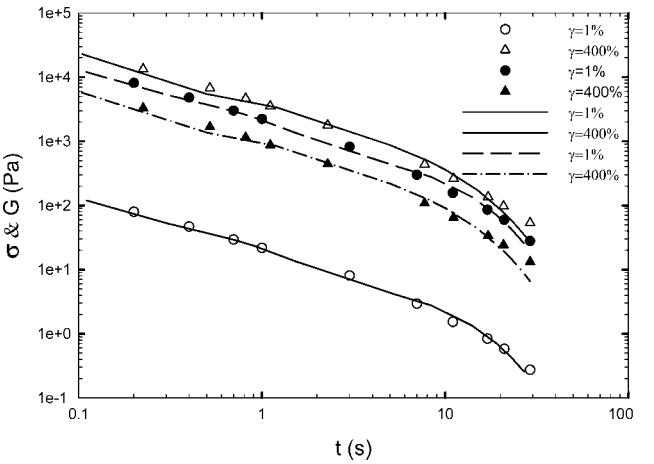

Figure 6 Stress σ and stress relaxation modulus *G* versus time *t*, as predicted with the UGM model, in single step-strain experiments. The symbols and lines are the same as described in Figure 4.

dramatically. In this work, we will compare the model predictions at the high strain value of 400%. Figure 2 illustrates that in the higher strain region, the relaxation moduli decrease and the stress increases with increasing strain. Theoretical results of stress and stress relaxation moduli were computed with the seven viscoelastic fluids models. The UMM, FCMM, UGM, UEWM, and FCMM–EWM model predictions are displayed in Figures 4–8. The PCMM and PCMM–EWM models performed similarly to the FCMM and FCMM–EWM models, respectively, and so are not presented for clarity.

Figure 4 demonstrates that the UMM model can predict the stress and stress relaxation modulus fairly well for the lower strain value, except that this model underpredicts both of them in the long-time region ($t > 19.5$ s). This implies that the UMM model does not have a large enough relaxation time resulting from the original parameter optimization, as already observed in ref. [1]. The UMM model overpredicts both the stress and the relaxation moduli at $\gamma = 400\%$ because this model cannot describe nonlinear viscoelastic responses.

Figures 5 presents the predictions of the FCMM model, which are qualitatively and quantitatively similar to those of the PCMM model. In the small-strain region, the model predicts the stress and modulus fairly well at small times but substantially underpredicts both at long times. For the higher strain value (400%), both the stress and modulus predictions are quite poor at all times. Note that the predictions of this model have a distinct waviness with respect to time. As explained before,[1,16,17] this behavior is

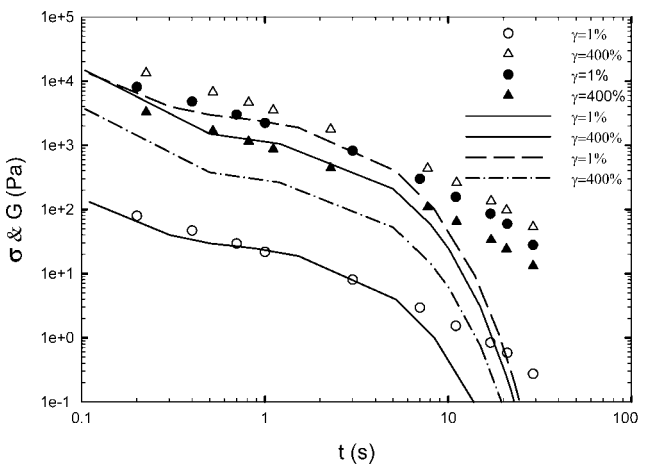

Figure 5 Stress σ and stress relaxation modulus *G* versus time *t*, as predicted with the FCMM model, in single step-strain experiments. The symbols and lines are the same as described in Figure 4.

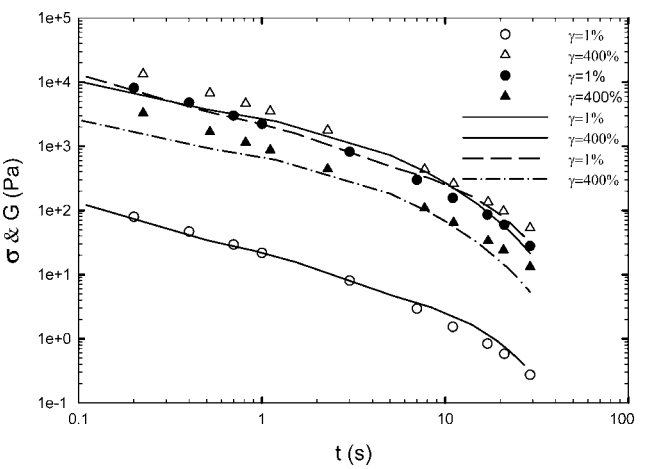

Figure 7 Stress σ and stress relaxation modulus *G* versus time *t*, as predicted with the UEWM model, in single step-strain experiments. The symbols and lines are the same as described in Figure 4.

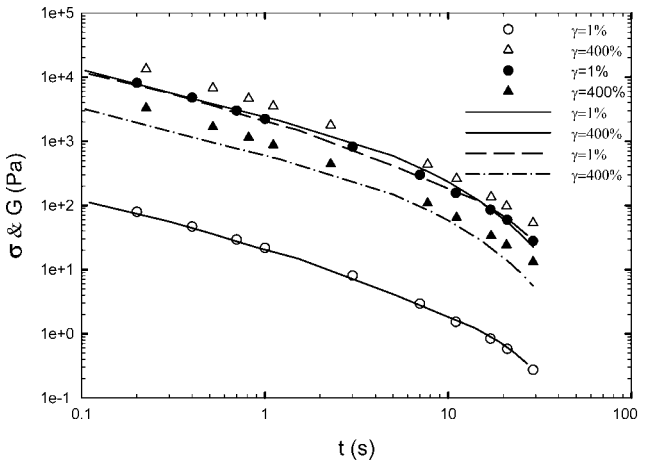

Figure 8 Stress σ and stress relaxation modulus *G* versus time *t*, as predicted with the FCMM–EWM model, in single step-strain experiments. The symbols and lines are the same as described in Figure 4.

caused by the unrealistic Maxwellian type of relaxation assumed by this model.

Figure 6 presents the theoretical predictions of the stress and modulus provided by the UGM model. This figure shows that the UGM model can describe the time variation of the stress and stress relaxation modulus fairly well for both small and large strain values, although some small deviations exist after about 20 s. Figure 7 displays the predictions of the UEWM model for the stress and modulus. The predictions for the lower strain value are very reasonable, but both the stress and modulus are underpredicted for all times at the higher strain value. In Figure 8, predictions for the stress and stress relaxation modulus from the FCMM–EWM model are compared to the experimental data. Good consistency is found between the predictions from the model and the experimental data for the lower strain, but for $\gamma = 400\%$, this model also underpredicts the stress and stress relaxation modulus over the entire time span. Predictions of the PCMM–EWM model (not shown) are similar qualitatively to those of the FCMM–EWM model but are not nearly as good quantitatively.

From Figures 3–8, we can conclude that (1) all the models examined herein can generally describe the evolution of the relaxation moduli with time at lower strain values and small times, (2) most of the models cannot capture the long-time behavior at small strains, and (3) the UGM model is the only one that can provide quantitative matches of the experimental data for high and low strains over the entire span of time.

Double step-strain experiments

Generally, there are two types of double step-strain experiments. Type I occurs when the total strain, γ_2, after the second applied strain is larger than the first applied strain, γ_1. Type II occurs when γ_2 is smaller than γ_1. The latter case is often called a reversing double step-strain experiment. We examined both types of double step-strain experiments. Because the performance of each model after the first step is virtually the same as that in a single step-strain experiment, except that the allowed time for the relaxation of the polymer melt is much shorter, we will focus our attention on times after the application of the second step. In all cases, the second step strain was applied at $t = 2$ s: we felt that this time was long enough for the small relaxation time modes to have fully relaxed (assuming no mode coupling), but not the long relaxation time modes. (Note that the relaxation times of each mode for all models can be found in refs. 1 and 16.)

Results of type I ($\gamma_2 > \gamma_1$) double step-strain experiments

In type I double step-strain experiments at low strain values, the comparison between model predictions and experimental data was very similar to that of the single step-strain experiments and will not be presented here. The interested reader can refer to ref. 16 for details.

The results for the stress computed with the UMM, PCMM, FCMM, and UGM models for the type I experiment ($\gamma_1 = 200\%$ and $\gamma_2 = 400\%$) are shown in Figure 9. Results from the UEWM, PCMM–EWM, and FCMM–EWM models are shown in Figure 10. The figures show a marked differentiation of the various models from one another to a degree not seen in the single step-strain experiments. The basic trends are the same as before, but the long-time behavior has been highly exaggerated. The UMM model overpre-

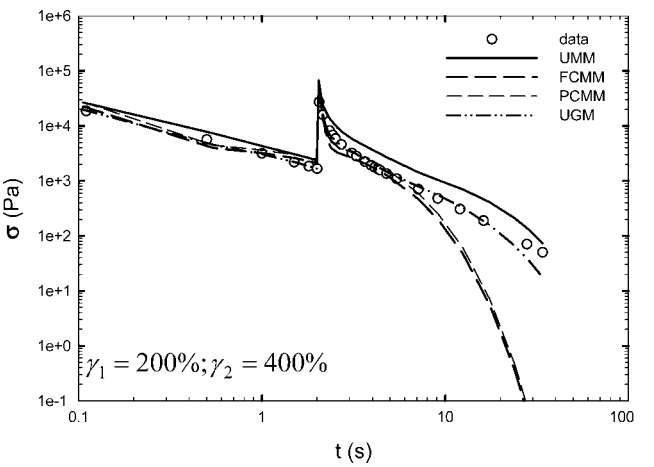

Figure 9 Stress σ versus time *t*, as predicted with the UMM, PCMM, FCMM, and UGM models, in double step-strain experiments at strains of $\gamma_1 = 200\%$ and $\gamma_2 = 400\%$.

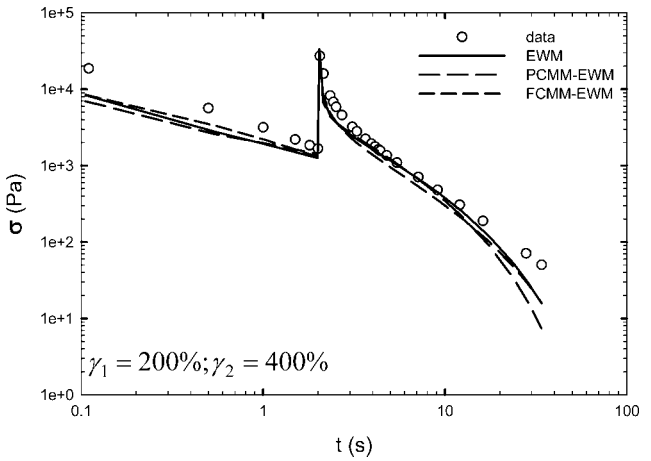

Figure 10 Stress σ versus time *t*, as predicted with the UEWM, PCMM–EWM, and FCMM–EWM models, in double step-strain experiments at strains of $\gamma_1 = 200\%$ and $\gamma_2 = 400\%$.

dicts the stress for all times, again because these large strain values lie outside the regime of linear viscoelasticity. The PCMM, FCMM, EWM, FCMM–EWM, and PCMM–EWM models all underpredict the experimental data to various degrees, with the FCMM and PCMM models again performing the worst, especially at long times. Only the UGM model gives an accurate prediction of the stress for all but the longest times. For this experiment, the UGM model is clearly the best of the seven.

Results of type II ($\gamma_2 < \gamma_1$) double step-strain experiments

From the previous subsection, it is clear that double step-strain experiments, at least at high strain values, can provide very critical tests of viscoelastic fluid models. That conclusion is emphasized in type II double step-strain experiments, even at small strain values. In this experiment, the stress can change sign at some point in time after the application of the second step strain because the direction of the strain has been reversed. Because the stress value right after the application of the second strain in a type II experiment changes sign, we present the absolute values of the stress as functions of time on a log–log scale. This turned out to be a very severe test of a viscoelastic fluid model to capture the point in time of this sign change.

In Figure 11, we give the performance of several models in type II double step-strain experiments for lower strain values ($\gamma_1 = 30\%$ and $\gamma_2 = 15\%$). The FCMM model predictions are very poor: The sign change of the stress is grossly underpredicted, as is the long-time experimental behavior. Again, this is in congruence with the results of part I,[1] which showed that this model was not particularly good at describing even steady-state nonlinear viscoelastic properties. The FCMM–EWM, UMM, and UGM models all offer surprising good predictions of the transient stress behavior for most points in time, although the UMM model does show significant deviations at long times. The PCMM, EWM, and PCMM–EWM models (not shown) all gave predictions resembling that of the FCMM model.[16]

Figures 12 and 13 present comparisons between the experimental data and model predictions of all seven models for the type II experiment at large strain values ($\gamma_1 = 400\%$ and $\gamma_2 = 200\%$). For this higher strain experiment, the models are greatly differentiated from one another. This occurs not only after the application of the second strain but also before its application, as discussed previously for the single step-strain experiments: many of the models cannot predict the

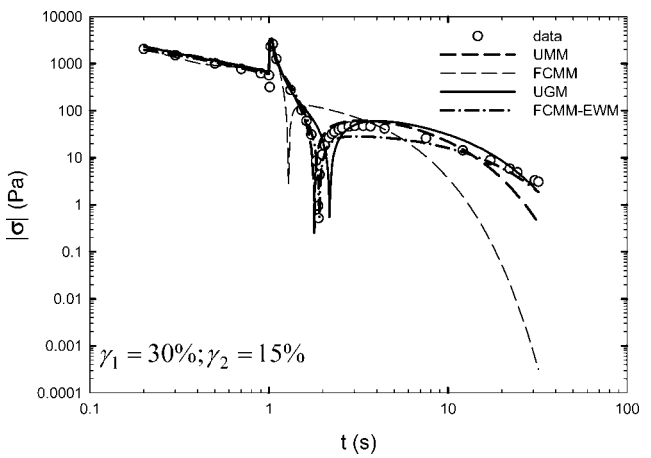

Figure 11 Stress σ versus time *t*, as predicted with the UMM, FCMM, UGM, and FCMM–EWM models, in double step-strain experiments at strains of $\gamma_1 = 30\%$ and $\gamma_2 = 15\%$.

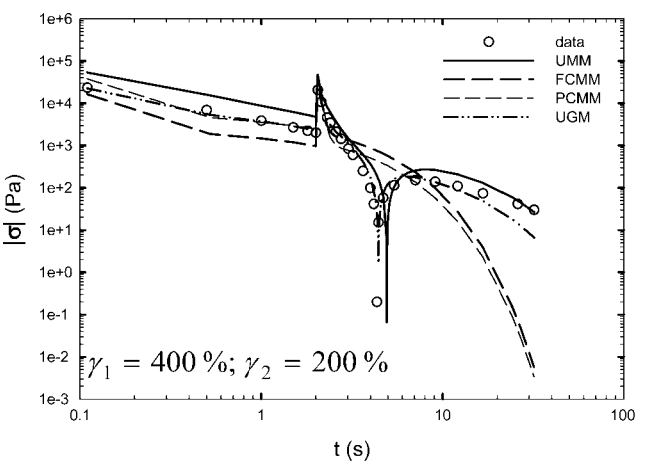

Figure 12 Stress σ versus time *t*, as predicted with the UMM, PCMM, FCMM, and UGM models, in double step-strain experiments at strains of $\gamma_1 = 400\%$ and $\gamma_2 = 200\%$.

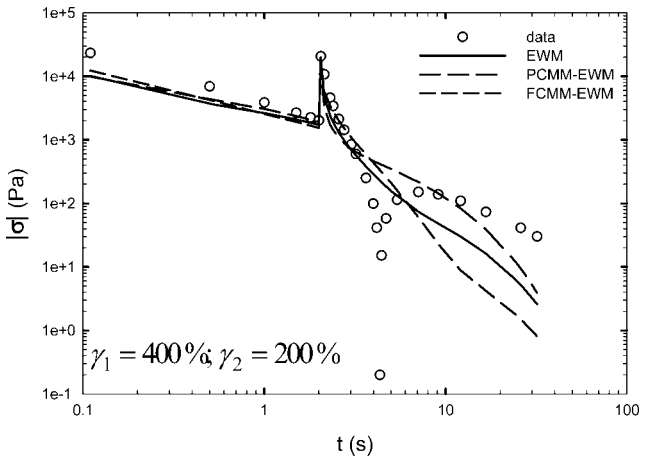

Figure 13 Stress σ versus time t, as predicted with the UEWM, PCMM–EWM, and FCMM–EWM models, in double step-strain experiments at strains of $\gamma_1 = 400\%$ and $\gamma_2 = 200\%$.

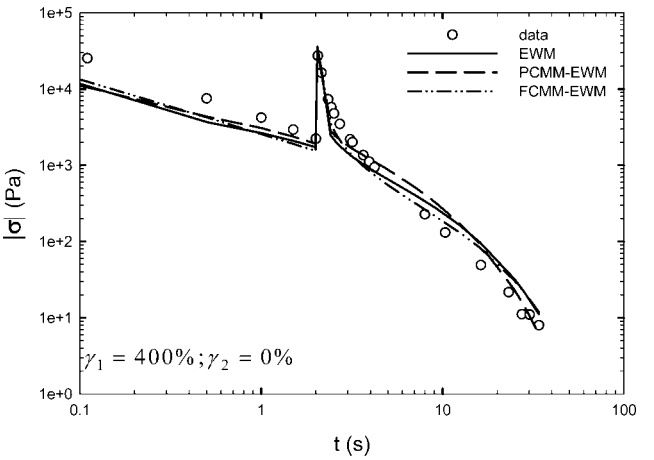

Figure 15 Stress σ versus time t, as predicted with the UEWM, PCMM–EWM, and FCMM–EWM models, in double step-strain experiments at strains of $\gamma_1 = 400\%$ and $\gamma_2 = 0$.

correct stress behavior for high strain values in the simpler experiment. Consequently, those models that could not predict the single step-strain experiment are at a disadvantage with respect to those that could do so.

In Figures 12 and 13, five of the seven models could not predict the sign change of the shear stress. Only the UMM and UGM models caught the sign change, the former rather paradoxically. The UGM model shows good agreement with the experimental data for all but the longest times and thus appears to be the best model of the seven examined. It is rather surprising that the FCMM–EWM model performs so poorly, given that it performed fairly well in the single step-strain and type I double step-strain experiments. We conjecture that the reason this model performs so poorly in this case is that the coupling effect between the modes causes the shorter relaxation time modes to activate at smaller times than their relaxation times would indicate and the longer time modes to activate at larger times.[18,19] This would effectively spread out the relaxation time spectrum, leaving a hole in the middle of the range; this would effectively blind the model to intermediate timescale relaxation phenomena.

Results of a special case ($\gamma_2 = 0$) in type II double step-strain experiments

In the special case ($\gamma_2 = 0$) of the type II double step-strain experiment, most polymeric fluids satisfy the consistency relation (called the Osaki–Kimura rela-

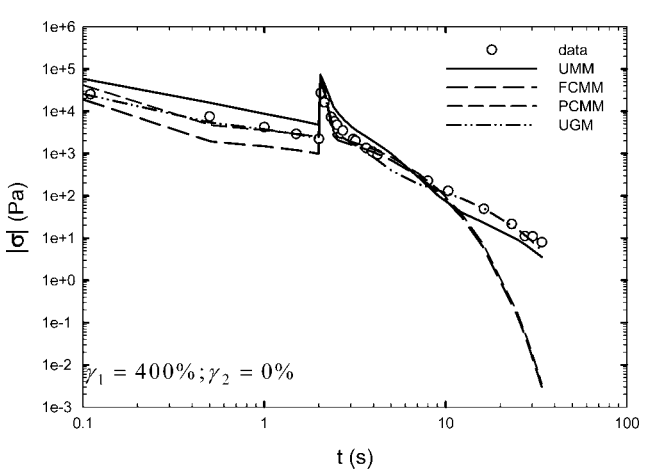

Figure 14 Stress σ versus time t, as predicted with the UMM, PCMM, FCMM, and UGM models, in double step-strain experiments at strains of $\gamma_1 = 400\%$ and $\gamma_2 = 0$.

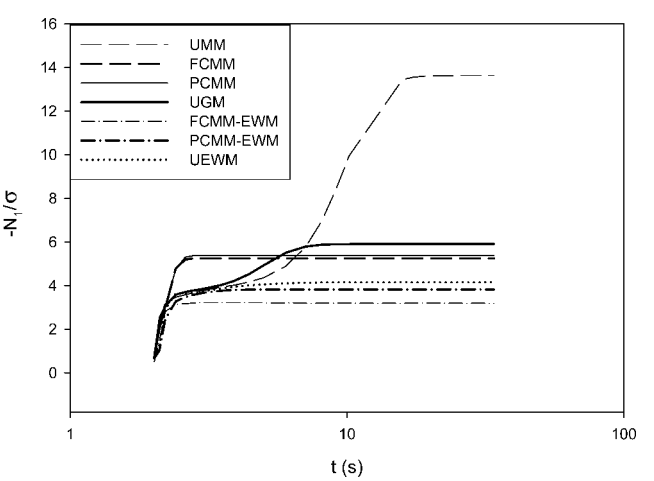

Figure 16 $-\frac{N_1(\gamma_1,t,t_1)}{\sigma(\gamma_1,t,t_1)}$ ratios predicted from the different models in the double step-strain experiment at strains of $\gamma_1 = 400\%$ and $\gamma_2 = 0$.

TABLE I
$-[N_1(\gamma_1,t,t_1)/\sigma(\gamma_1,t,t_1)]$ Ratios from the Different Models (the Long-Time Asymptotes) in the Double Step-Strain Experiments at Strains of $\gamma_1 = 400\%$ and $\gamma_2 = 0$

Model	UMM	PCMM	FCMM	UEWM	PCMM–EWM	FCMM–EWM	UGM
$-\frac{N_1(\gamma_1,t,t_1)}{\sigma(\gamma_1,t,t_1)}$	13.6	5.38	5.25	4.15	3.82	3.19	5.90

tion) $-\frac{N_1(\gamma_1,t,t_1)}{\sigma(\gamma_1,t,t_1)} = \gamma_1$, where $N_1(\gamma_1,t,t_1)$ is the first normal stress difference and $\sigma(\gamma_1,t,t_1)$ is the shear stress after the second strain is applied.[20,21] Here, we checked this consistency relationship for our polymer melt. Unfortunately, we could not obtain the experimental data for the first normal difference in the double step-strain experiment because of device limitations. What we could do, however, was to check whether the predictions of the different models obeyed this consistency relation.

The results of the stress predicted with the UMM, PCMM, FCMM, and UGM models for the type II experiment ($\gamma_1 = 400\%$ and $\gamma_2 = 0$) are shown in Figure 14. The corresponding results from the UEWM, PCMM–EWM, and FCMM–EWM models are shown in Figure 15. The shear stress is plotted as the absolute value of the stress as a function of time in Figures 14 and 15. The values of the stress are negative after the application of the second strain. Figures 14 and 15 demonstrate that all the models can give a good prediction for the largest absolute value of the negative stress. Also, all the models can generally describe the trend of the stress evolution with time. The stress from the PCMM and FCMM models demonstrates some waviness, as usual, and both of these models underpredict the stress for long times. The UEWM, PCMM–EWM, and FCMM–EWM models give fair predictions after the strain returns to its original position, although they underpredict the stress in the first strain region. The UGM model again performs very well throughout the course of the experiment.

In Figure 16, we plot the ratio $-\frac{N_1(\gamma_1,t,t_1)}{\sigma(\gamma_1,t,t_1)}$ as a function of time after the second strain is applied for all seven models. This ratio increases right after the second strain is applied and then reaches a steady-state value after a certain amount of time has elapsed (which is different for each model). In Table I, we list the steady-state value of this ratio. From the Osaki–Kimura relation, this ratio should be γ_1, and, in this case, its value should be 4.0. From Table I, we see that the UMM model gives an outrageously high prediction, whereas the others predict values between 3.19 and 5.90.

CONCLUSIONS

Single and double step-strain experiments are powerful tools for examining viscoelastic constitutive equations. Seven constitutive equations were tested against experimental data from these experiments after the fitting of the requisite parameters in part I.[1] In general, most models could predict well experimental data of the single step-strain experiment at small strain values and short times, but most of these had difficulty at long times. For higher strain values, most models gave incorrect predictions for the data, with the exception of the UGM model. In the double step-strain experiments, only the UGM model could faithfully capture the short- and long-time behavior of the polymer melt for both low and high strains. Indeed, the UGM model even outperformed the FCMM–EWM model, which contains roughly twice as many parameters.[1] Thus, it appears that the quadratic relaxation behavior present in the UGM model is very important for describing the experimental data of real polymer melts and that the mode-coupling effect is of secondary importance.

Although not reported herein, we also examined the effects of replacing the linear elastic spring behavior in each of the seven models with finitely extensible nonlinear elastic spring forces (FENE-P springs). This turned out not to have an effect on the model predictions in most of the flows of ref. 1 and this article, even though the number of parameters increased accordingly. Details of this additional work can be found in ref. 16.

References

1. Jiang, B.; Kamerkar, P. A.; Keffer, D. J.; Edwards, B. J. J Appl Polym Sci 2006, 99, 405.
2. Ferry, J. D. Viscoelastic Properties of Polymers; Wiley: New York, 1980.
3. Phan-Thien, N.; Tanner, R. I. J Non-Newtonian Fluid Mech 1977, 2, 353.
4. Apelian, M. R.; Armstrong, R. C.; Brown, R. A. J Non-Newtonian Fluid Mech 1988, 27, 299.
5. Souvaliotis, A.; Beris, A. N. J Rheol 1992, 36, 241.
6. Giesekus, H. J Non-Newtonian Fluid Mech 1982, 11, 69.
7. Goublomme, A.; Draily, B.; Crochet, M. J. J Non-Newtonian Fluid Mech 1992, 44, 171.
8. Crochet, M. J.; Goublomme, A. J Non-Newtonian Fluid Mech 1993, 47, 281.
9. Bernstein, B.; Kearsley, E. A.; Zapas, L. J. Trans Soc Rheol 1963, 7, 391.
10. (a) Doi, M.; Edwards, S. F. J Chem Soc Faraday Trans 2 1978, 74, 1789; (b) Doi, M; Edwards, S. F. J Chem Soc Faraday Trans

2 1978, 74, 1802; (c) Doi, M; Edwards, S. F. J Chem Soc Faraday Trans 2 1978, 74, 1818.
11. Larson, R. G. Constitutive Equations for Polymer Melts and Solutions; Butterworths: Boston, 1988.
12. Venerus, D. C.; Kahvand, H. J Polym Sci Part B: Polym Phys 1994, 32, 1531.
13. Wagner, M. H.; Ehrecke, P. J Non-Newtonian Fluid Mech 1998, 76, 183.
14. Chodankar, C. D.; Schieber, J. D.; Venerus, D. C. J Rheol 2003, 47, 413.
15. Li, W. H.; Du, H.; Yeo, G. H.; Guo, N. Q. Smart Mater Struct 2002, 11, 209.
16. Jiang, B. Ph.D. Dissertation, University of Tennessee, 2005.
17. Jiang, B.; Kamerkar, P. A.; Keffer, D. J.; Edwards, B. J. J Non-Newtonian Fluid Mech 2004, 120, 11.
18. Edwards, B. J.; Mavrantzas, V. G.; Beris, A. N. J Rheol 1996, 40, 917.
19. Beris, A. N.; Edwards, B. J. Thermodynamics of Flowing Systems; Oxford University Press: New York, 1994.
20. Venerus, D. C.; Kahvand, H. J Rheol 1994, 38, 1297.
21. Osaki, K.; Kimura, S.; Kurata, M. J Rheol 1981, 25, 549.